Research Article

Ghada ALMisned, Elaf Rabaa, Duygu Sen Baykal, Erkan Ilik, Gokhan Kilic, Hesham M. H. Zakaly, Antoaneta Ene*, Huseyin Ozan Tekin*

Translocation of tungsten(VI) oxide/gadolinium(III) fluoride in tellurite glasses towards improvement of gamma-ray attenuation features in high-density glass shields

https://doi.org/10.1515/chem-2022-0289
received January 27, 2023; accepted February 9, 2023

Abstract: This study investigates the effect of substituting tungsten(VI) oxide/gadolinium(III) fluoride in tellurite glasses whose densities varies from 5.0879 to 5.3246 g/cm^3 on gamma-ray absorption properties. A range of fundamental absorption parameters, including attenuation coefficients, half-value layer thicknesses, effective atom and electron numbers, effective conductivity, exposure, and energy absorption buildup factors, were studied for five different glass samples with varying substitution ratios. The ratio of tungsten(VI) oxide to gadolinium(III) fluoride varied between 0 and 20 mol%, as well as the TeO_2 ratio in the composition was maintained between 90 and 80 mol%. The sample with the composition of 80–20 mol% TeO_2/WO_3, which attained the maximum density value with 20 mol% WO_3 addition, showed the highest gamma-absorption capabilities based on the obtained findings in the range of 0.015–15 MeV. In consideration of the mechanical and physical properties of WO_3 in tellurite glasses, it can be concluded that WO_3 incorporation is a crucial monotonic process that may be utilized to further improve the properties of glass shields.

Keywords: tellurite glasses, GdF_3, WO_3, gamma-ray, glass shields

1 Introduction

Ionizing radiation is one of the natural phenomena that people encounter on a daily basis, coming from outer space, the air, and the earth; yet, in recent years it has also become a man-made phenomenon with medical, industrial, and commercial processes [1–5]. Nuclear research, agriculture, and food technology have benefited from the radiation industry's innovative applications [6,7]. However, there are risks to the environment and human health linked with the use of ionizing radiation in addition to its advantages. In addition to the benefits of employing alpha, gamma, and X-rays in medical applications, the detrimental radiation effects may result in severe chromosomal abnormalities and carcinogenic consequences [8–10]. Ionizing radiation is considered to cause harmful damage to living tissues in direct and indirect ways by changing cell structure and damaging their genetic material (DNA). Radiation damage depends on the sensitivity of an organ as well as the amount of energy and type of radiation being absorbed, whether it was due to exposure to high levels of radiation, which would have an immediate effect, or stochastic effects, which are probabilistic and can

* **Corresponding author: Antoaneta Ene,** INPOLDE Research Center, Department of Chemistry, Physics and Environment, Faculty of Sciences and Environment, Dunarea de Jos University of Galati, 47 Domneasca Street, 800008 Galati, Romania, e-mail: Antoaneta.Ene@ugal.ro
* **Corresponding author: Huseyin Ozan Tekin,** Medical Diagnostic Imaging Department, College of Health Sciences, University of Sharjah, Sharjah, 27272, United Arab Emirates; Computer Engineering Department, Faculty of Engineering and Natural Sciences, Istinye University, Istanbul 34396, Turkey, e-mail: tekin765@gmail.com
Ghada ALMisned: Department of Physics, College of Science, Princess Nourah Bint Abdulrahman University, P.O. Box 84428, Riyadh 11671, Saudi Arabia
Elaf Rabaa: Medical Diagnostic Imaging Department, College of Health Sciences, University of Sharjah, Sharjah, 27272, United Arab Emirates
Duygu Sen Baykal: Vocational School of Health Sciences, Istanbul Kent University, Istanbul 34433, Turkey
Erkan Ilik, Gokhan Kilic: Department of Physics, Faculty of Science, Eskisehir Osmangazi University, Eskisehir, 26040, Turkey
Hesham M. H. Zakaly: Institute of Physics and Technology, Ural Federal University, 620002 Ekaterinburg, Russia; Physics Department, Faculty of Science, Al-Azhar University, Assiut 71524, Egypt

occur at unexpected times during increasing radiation exposure. For this reason, scientific researchers have focused on the importance of radiation shielding and radiation protection [11–14]. Different materials have been used to protect against radiation by blocking its initial intensity to a degree that is not harmful [15–17]. In addition to other principles and guidelines for radiation protection, such as reducing exposure duration and increasing distance from the radiation source, shielding materials are considered to be the most beneficial method along with the rest [18–20]. Conventional lead (Pb) and other materials such as tungsten, antimony, and barium are typically used for protection shielding materials such as clothes for medical personnel and patients going under radiation [21–24]. In recent years glass materials [25–27] proved to show efficient radiation protection properties and applications. Due to its transparency, high thermal stability, and permeability, as well as the ease with which it can be fabricated and shaped. Many scientists and engineers have taken these advantages into consideration to utilize glass materials as optical and radiation shielding applications [28–30]. After witnessing the drawbacks of conventional shielding materials such as Pb and concrete [31,32], glass materials have shown to be non-toxic and have a high level of endurance, making them an intriguing option for shielding investigation and development [33]. Tellurite glass compared to other glass materials have showed interesting features such as gain high density, transmission of infrared, low melting temperature, and high dielectric constant [34]. Our goal in this research is to investigate the physical and optical properties of TeO_2 with WO_3 and GdF_3 [35], since tellurite glass needs secondary ingredient to form glasses [36]. In this study, WO_3 was chosen because of its anti-crystallization ability as well as to improve the glass transition temperature [37]. The GdF_3 is used in this research as it is widely employed as a host for fluorescents thanks to its various outstanding material properties during the glass manufacturing process [38,39]. In the TeO_2–WO_3–GdF_3 glass system [35] five different types of glasses have been prepared in variable proportions with WO_3 as a different glass former and GdF_3 as a modifier. The first and second samples were formed by adding 80 mol% of TeO_2 and varying the WO_3 and GdF_3 compositions (mol%) to achieve different densities, by adding in the first sample 10 mol% of WO_3 while keeping GdF_3 at a stable 0 mol%, and in the second sample, we have reversed the compositions process by keeping the WO_3 at a stable 0 mol% and adding 10 mol% of GdF_3, as shown in Table 1. By altering the mol% composition of the five glass samples, various densities were determined to investigate the optimum composition of the TeO_2–WO_3–GdF_3 glass system, in addition to identifying the glass system with the best radiation protection qualities.

Table 1: Density values and glass compositions of samples [35]

Glass code	Glass composition (mol%)	Density (g/cm^3)
G1	$90TeO_2$–$0WO_3$–$10GdF_3$	5.0879
G2	$90TeO_2$–$10WO_3$–$0GdF_3$	5.1231
G3	$80TeO_2$–$0WO_3$–$20GdF_3$	5.3115
G4	$80TeO_2$–$10WO_3$–$10GdF_3$	5.3246
G5	$80TeO_2$–$20WO_3$–$0GdF_3$	5.3355

This study's extensive findings may contribute to the comprehension of the absorption characteristics of WO_3-doped tellurite glasses. In addition, the results of this study may provide a comprehensive analysis with comparable glass compositions published in the literature, therefore facilitating the employment of the most appropriate material structures into radiation protection process through glass shields.

2 Materials and methods

Using five designed samples of varied compositions of the TeO_2–WO_3–GdF_3 glass system [35], we determined numerous essential gamma-ray shielding parameters in this study. The five different samples designated G1, G2, G3, G4, G4, and G5 for this investigation were previously synthesized using the conventional melt-quenching method. In this study, gamma-ray absorption properties were examined in the range of 0.015–15 MeV using Py-MLBUF [40] software to conclude gamma ray absorption parameters. Next, they were displayed using the ORIGIN2018 software. The linear attenuation coefficients, half-value thickness, and mean free path lengths were obtained and examined as a function of energy for each glass sample. In addition, exposure and energy absorption buildup factors were also calculated in the 0.015–15 MeV energy range over a broad variety of mean free path values, ranging from 0.5 to 40 mfp. From our previous studies [41] and other published works [42,43], one may acquire more comprehensive technical information and theoretical calculation approaches related to these determined critical parameters for the current glasses.

3 Results and discussion

In this study, five different composition samples of TeO_2–WO_3–GdF_3 glass system were taken under investigation

for gamma-ray absorption parameters. Gamma-ray absorption properties were taken through critical calculation software separately. In many instances, the density of materials used to absorb ionizing gamma and X-rays correlates with their absorption characteristics. The tendency for the incoming radiation to be absorbed through internal interactions and interact with more electrons explains how high-density materials are more effective at absorbing this type of radiation. This investigation has revealed that the five analyzed samples had varying densities. Figure 1 depicts the density of the tested glass samples. As can be seen, the G5 sample, which contains 20 mol% of WO_3 and 80 mol% of TeO_2, has the maximum glass density value at 5.3355 g/cm^3. In this example, TeO_2 has the lowest concentration while WO_3 has the highest concentration among the studied glass samples. The quantitative changes in the calculated gamma-ray absorption characteristics will be determined as a function of the density change as a result of the WO_3 incorporation into glass system, which is the primary objective of this study. In the gamma-ray absorption parameters, first, linear attenuation coefficients were calculated in the energy range of 0.015–15 MeV. The μ values can be calculated through a typical transmission setup (Figure 2). The intensity of incident gamma-ray beam would change as a function of absorber thickness as well as linear attenuation coefficient (μ) value of the absorber at a certain energy. Figure 3 depicts the variation in linear attenuation coefficient (μ) of the five analyzed glass samples as a function of increasing energy. The reported changes in μ values reflect the behavior of the incident photon, whether it was partially absorbed, and the other half was dispersed, or whether it was completely absorbed by the electrons on the atomic orbits. It seems that photons in low energies were greatly affected from photoelectric effect, which explains the high attenuation values in the lower energies. As energy increased, the Compton scatter effect subsequently increased. The graph shows a sharp drop between 0.01 and 0.03 MeV, then an incline approximately after 0.04 MeV. Through the drop and rise in the low energies, a steady decrease appeared from 0.05 to 8 MeV. Our results showed that G5 sample with the maximum WO_3 and minimum TeO_2 contribution in its composition has the highest μ values at almost all energy levels. As seen in Figure 3, there were also some minor deviations around the k-absorption edge points of the samples. However, it is likely that an increase in WO_3 doping in telluride glasses may have a similar effect on the linear attenuation coefficients. Another gamma-ray shielding parameter, which is a density-independent parameter, is known as mass attenuation coefficient (μ_m). This

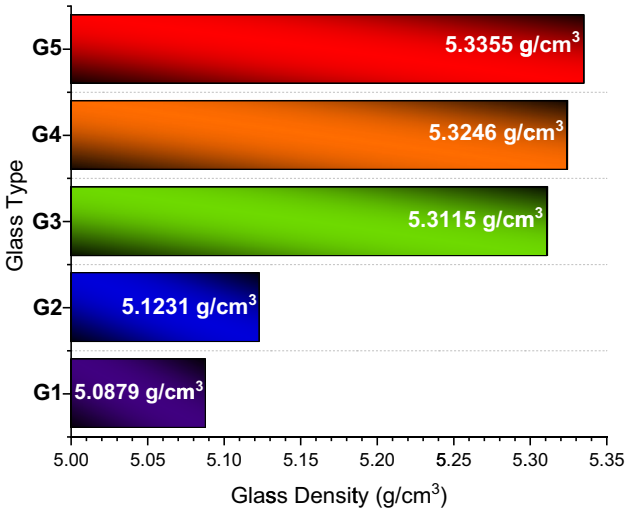

Figure 1: Variation of investigated glass densities.

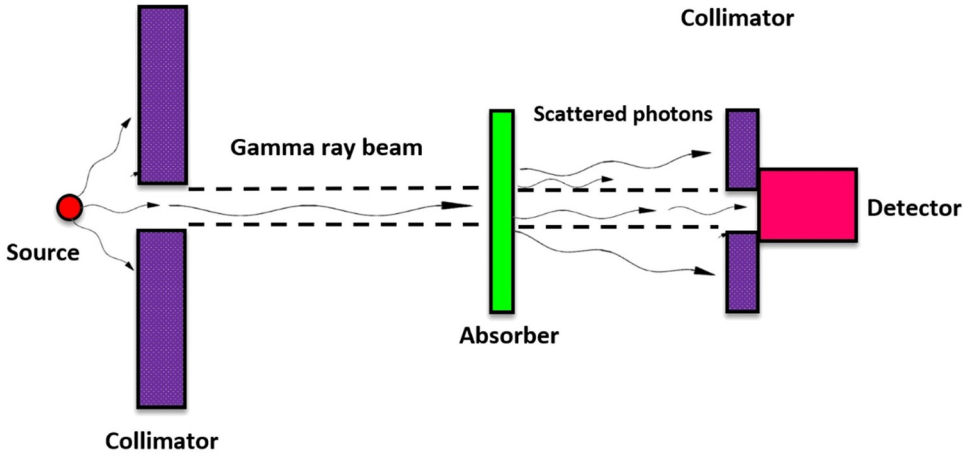

Figure 2: A typical setup for gamma-ray transmission measurements.

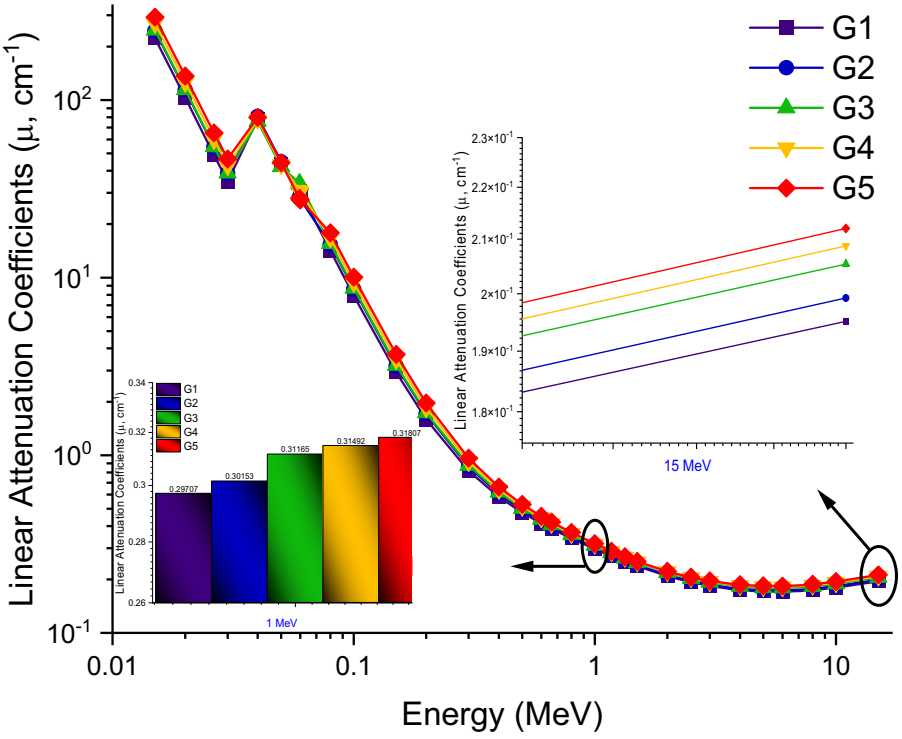

Figure 3: Variation of linear attenuation coefficient (cm^{-1}) with photon energy (MeV) for all G1–G5 glasses.

parameter provides crucial data on the absorber's partial removal of incident gamma-rays per unit mass. Due to the larger atomic number of W in WO_3, 20 mol% doping has enhanced the μ_m values of G5. Figure 4 displays the change of μ_m values between 0.015 and 15 MeV. As seen, the fluctuation of μ_m values was influenced by photon–

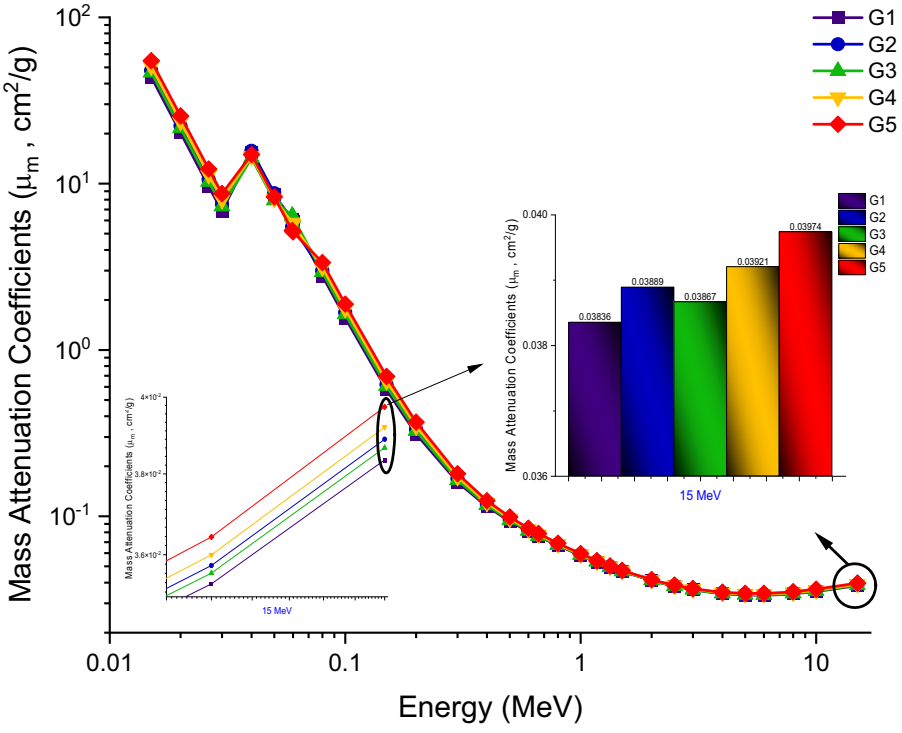

Figure 4: Variation of mass attenuation coefficients (cm^2/g) with photon energy (MeV) for all G1–G5 glasses.

matter interactions and, therefore, photon energy regions. Maximum μ_m values were recorded at low energies and vice versa. The G5 sample, with the maximum contribution of WO_3, was reported with the highest μ_m values. The atomic weight and density of the G5 sample allow it to have maximum linear and mass attenuation coefficient values within the range of 0.015–15 MeV. Half-value layer (HVL) is an essential parameter in investigating radiation-shielding material, which represents the minimum thickness of the radiation shielding required to decrease its primary energy to its half value [13]. If the thickness of the absorber remains in low levels, the efficiency of the material is proven to be more effective at attenuating the energetic photons. The graph seen in Figure 5 shows the relationship of the five glass samples with respect to HVL at a certain energy. As the energies start to increase, the HVL values increase as well, showing variation levels of values between the five samples, where G5 have the lowest HVL which give it advantages for determining radiation shielding materials. It is well-known that the linear attenuation coefficient has an inverse relationship with HVL. Eventually, it is a reasonable explanation for the low HVL sample to have high linear attenuation coefficient. For example, HVL values were reported as 3.5519, 3.4789, 3.3747, 3.3203, and 3.2688 cm for G1, G2, G3, G4, and G5 samples at 15 MeV, respectively. Accordingly, it can be said that G5, due to its greatest WO_3 contribution in the structure, would reduce the intensity of incoming photons to the lowest maximum thickness among the glass samples studied. On the other hand, mean free path values is another parameter that the result should be as low as possible, which represent the average path of a moving radiation between collisions, that would modify its direction or energy, in addition prove the ability of attenuation in a material. Lower mfp values for an attenuator material may be regarded as a good indicator of absorption if two consecutive interactions are conducted at short ranges. As illustrated in Figure 6, G5 was reported to have the lowest mfp value along with increasing energy. This can be considered as another positive effect of WO_3 on gamma-ray attenuation properties of glasses [44]. Another important parameter to discuss is the effective atomic number (Z_{eff}) values of shielding materials [16]. It is well-known that the number of electrons in the atomic orbit is related to Z number in the nucleus. Therefore, it is likely that atoms with higher Z values would also have a higher number of electrons, and incoming photons may be more likely to collide with electrons. The higher the collision, the greater the percentage of absorption due to the released energy of incoming photons in every collision with electrons [16,22],

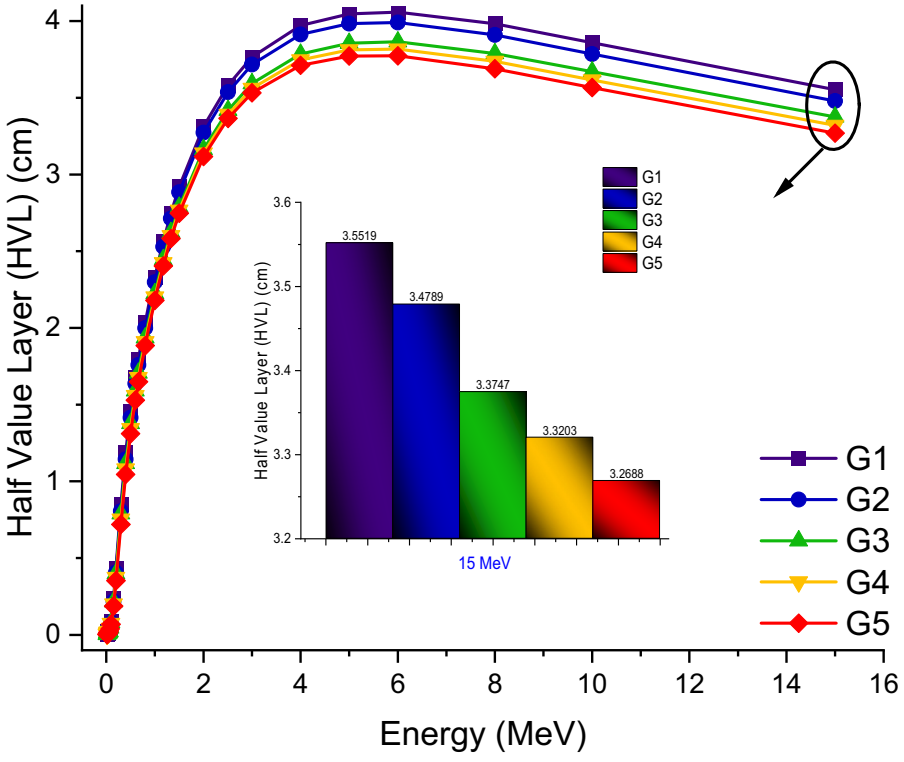

Figure 5: Variation of HVL (cm) with photon energy (MeV) for all G1–G5 glasses.

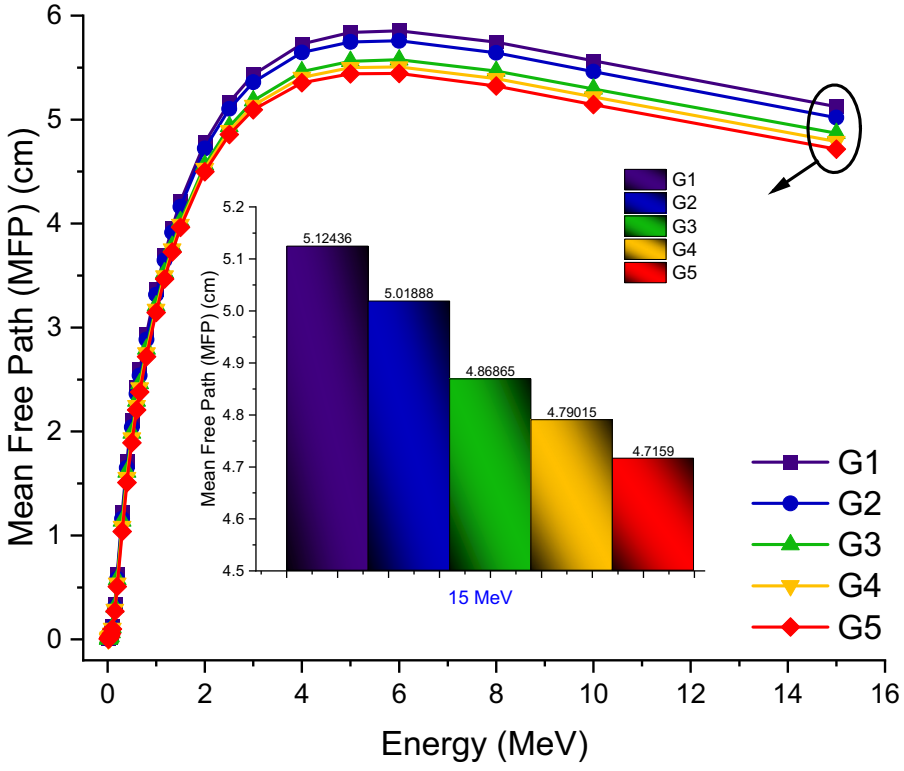

Figure 6: Variation of mean free path (cm) with photon energy (MeV) for all G1–G5 glasses.

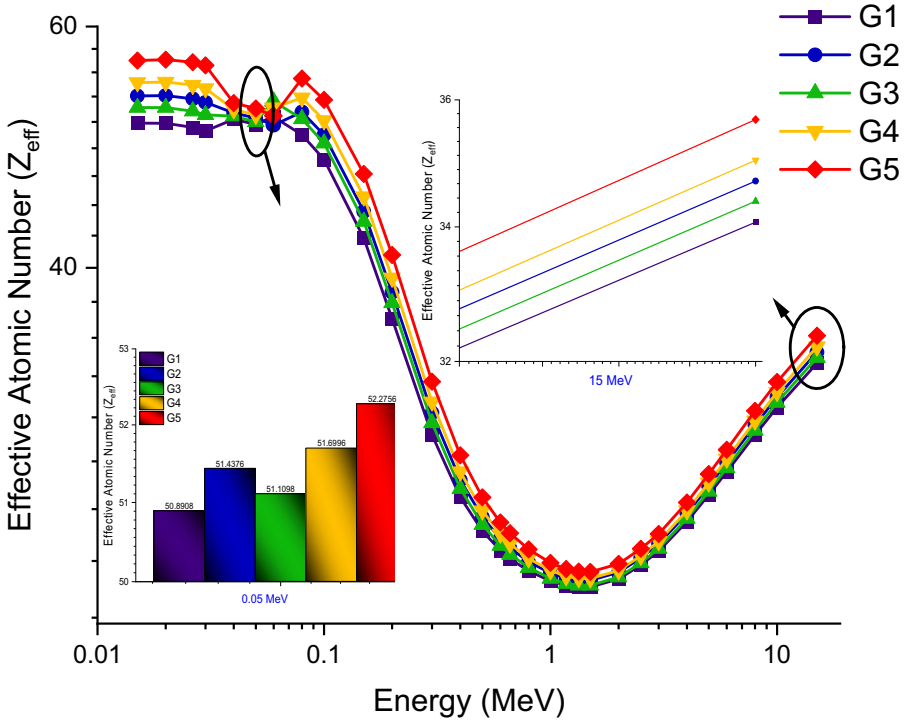

Figure 7: Variation of effective atomic number (Z_{eff}) with photon energy (MeV) for all G1–G5 glasses.

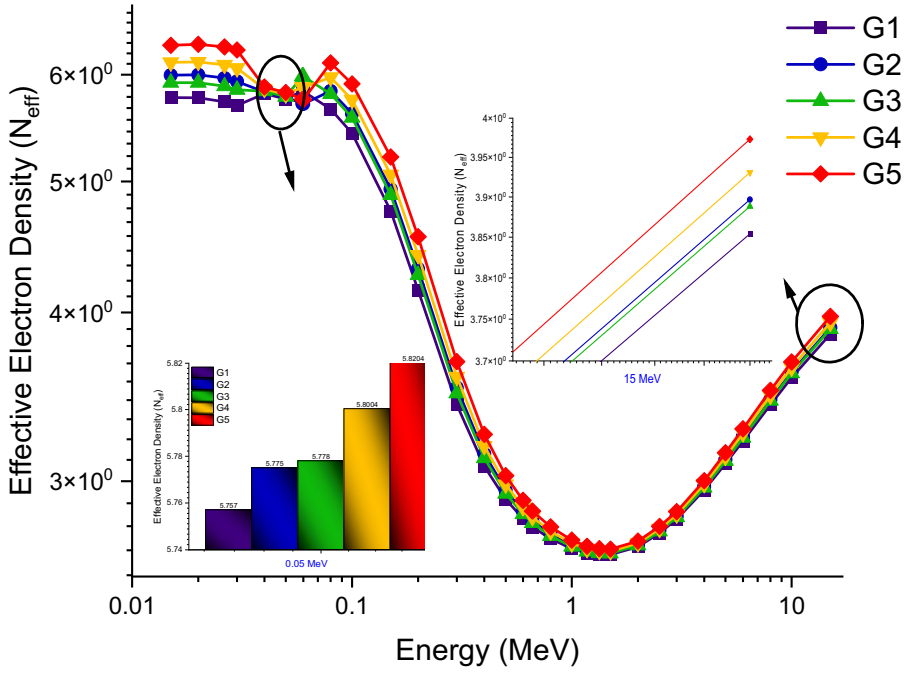

Figure 8: Variation of effective conductivity (C_{eff}) with photon energy (MeV) for all G1–G5 glasses.

which may result in either an excitation or the electron dropping off its orbit. The variation of effective atomic number (Z_{eff}) as a function of increasing energy is shown in Figure 7 for G1, G2, G3, G4, and G5 samples. The G5 structure, which has 20 mol% WO_3 doping, possesses the highest Z_{eff} values. This is due to the larger Z number of W, which has been translocated with Te in the glass structure. Therefore, one might anticipate an overall increase in G5's

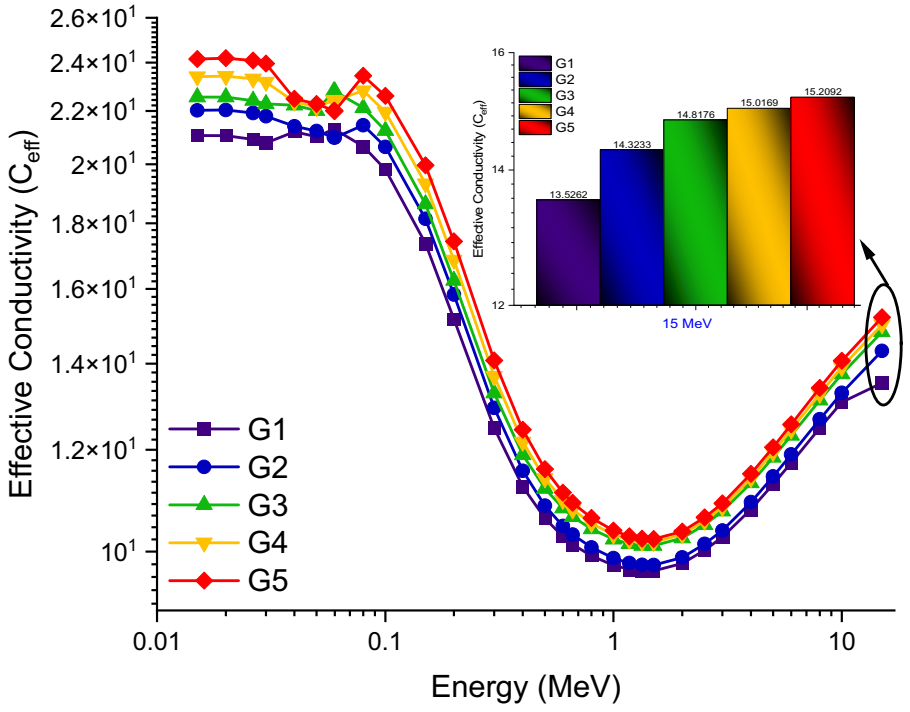

Figure 9: Variation of effective electron density (electrons/g) with photon energy (MeV) for all G1–G5 glasses.

Z number, which has a clear advantage over G1. Figure 8 represents the effective conductivity (C_{eff}) variation in all glass samples, where a clear and rapid decrease occurs while increasing the photon energy, mainly in the region where the photoelectric effect is dominant. G5 was the sample with the greatest C_{eff} values at all energies among those examined. This may be attributed to the growing number of electrons in the G5 sample because of the addition of elements with a high Z number. Since the conductivity level is the result of electron mobility between atoms, one may anticipate that the highest C_{eff} values of the G5 sample also reflect an increase in the number of electrons in the structure of G5. Figure 9 clearly depicts the changes in the number of electrons, which are the primary reason for the C_{eff} parameter findings. Figure 8 depicts the variation in the effective electron density (N_{eff}) values of the examined glass samples as a function of energy. The change in electron value owing to the Z increase indicated in the previous section was seen as an upward trend in the N_{eff} value from G1 to G5, with the highest values found for

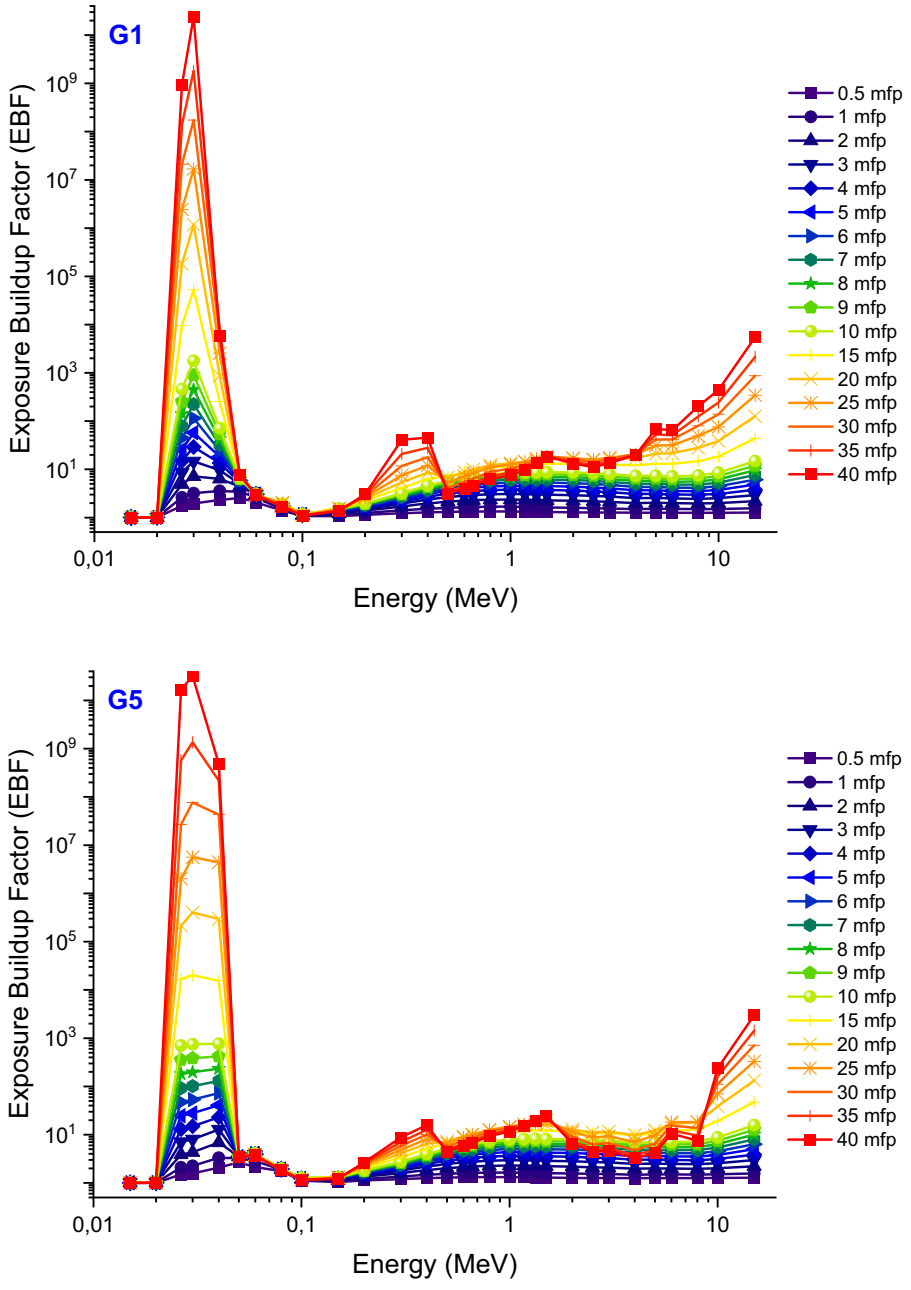

Figure 10: Variation of EBF of G1 and G5 glasses at different mean free path values.

G5. Electrons play a well-known role in the interaction of gamma rays with matter. The quantity of interaction in the G5 glass is likely to be the largest of the five investigated glasses, since more electrons would produce more interaction probabilities; this is a significant result pertaining to the G5's superior absorption features. The buildup factor also serves as a good approximation, and its low values suggest that the absorption process of the material in the calculated mean free path values is outstanding [45].

Figures 10 and 11 display the variation of computed exposure build-up factor (EBF) and energy absorption build-up factor (EABF) values for G1 and G5 glasses containing 0 and 20 mol% WO_3 at different mfp values from 0.5 to 40, respectively. The EBF and EABF values of the sample without the WO_3 additive are much greater compared to the sample with 20% WO_3, as shown in Figures 10 and 11. This is a consequence of the 20 mol% TeO_2/WO_3 translocation and demonstrates improved absorption properties.

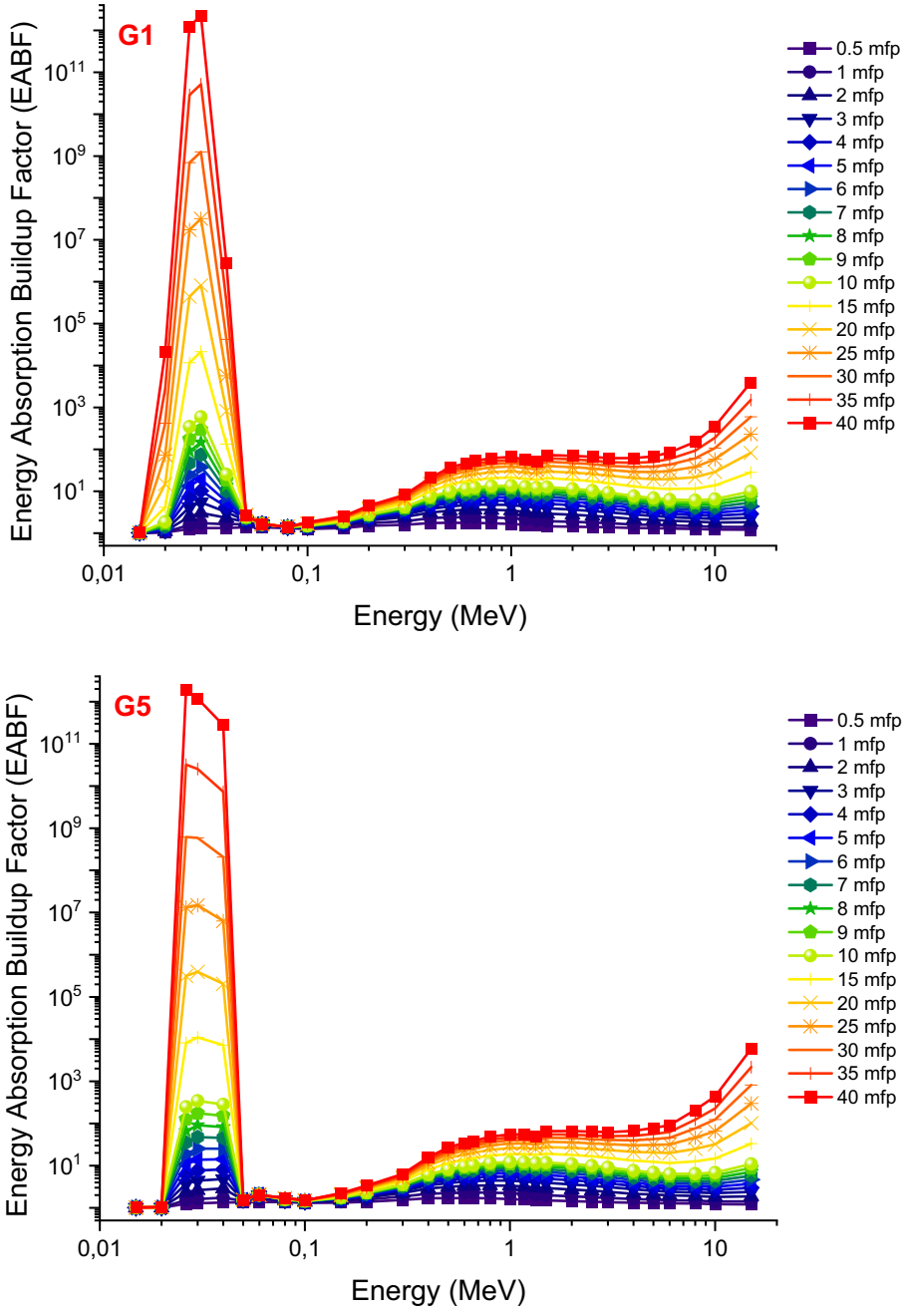

Figure 11: Variation of EABF of G1 and G5 glasses at different mean free path values.

This suggests that the rate of photon interactions in the glass doped with 20 mol% WO_3 is high. As is well-known, a large number of contacts between the incident photon and attenuator material is a vital signal that the absorption process would progress at a quicker pace, quantitatively [46–52]. Overall calculated absorption properties for energetic photons were found to be consistent, and 20 mol% WO_3-doped glass (i.e., G5) was shown to be the optimum composition for absorbing energetic gamma rays among the investigated glass samples.

4 Conclusion

High-density glasses prepared using the conventional melt-quenching method have become the focus of many researchers in terms of their radiation shielding capacity. Based on the work in which amorphous glass structures were synthesized before, the ability to control glass densities relatively by changing the additive ratio is very valuable in terms of minimizing the destructive effects of radiation. The gamma ray attenuation parameters were investigated in this study for the TeO_2–WO_3–GdF_3 glass system. Glass materials have shown to be nontoxic and have a high level of endurance, making them an intriguing option for shielding investigation and development where many scientists and engineers have taken these advantages into considerations to utilize glass materials as optical and radiation shielding applications. Tellurite glass has attracted strong interest as a possible component for lasers, fibers, and nonlinear optical systems for its potential properties and high density. An investigation of the radiation shielding properties for the five glass samples were obtained with a broad spectrum of input photon energies in order to compare the nuclear attenuation shielding capabilities. Between the five sample G5 showed to have the highest density of 5.3355 (g/cm^3) while the rest of the glass samples varies from 5.0879 to 5.3246 (g/cm^3). MAC values at an energy of 0.8 MeV for G1, G2, G3, G4, and G5 samples were 0.066942, 0.067696, 0.067404, 0.068158, and 0.068911, making G5 the prominent sample. Moreover, throughout the investigation of HVL values, G5 was the prominent of having the least HVL value through the whole spectrum of photon energies. Furthermore, both the (Z_{eff}) and (C_{eff}) values in G5 sample were the highest of all samples. Making it more efficient at absorbing the incident photon energy as well as a potential option for gamma radiation shielding materials. In this study, it is an important result that WO_3 in the glass composition increases the effective atomic number of the glasses and significantly reduces the mean free path. Considering that the radiation shielding capabilities of the element changes, it was clearly seen from the results of this study that the WO_3-doped glass structures exhibit superior properties On the other hand, thanks to new features such as optical band gap and glass densities added to glasses, it may be possible to gain new materials in various application areas. It is also an important factor that the glasses used as alternative radiation shielding materials are non-toxic compared to pure Pb or PbO-doped materials.

Acknowledgements: The authors would like to express their deepest gratitude to Princess Nourah bint Abdulrahman University Researchers Supporting Project number (PNURSP2023R149), Princess Nourah bint Abdulrahman University, Riyadh, Saudi Arabia.

Funding information: Princess Nourah bint Abdulrahman University Researchers Supporting Project number (PNURSP2023R149), Princess Nourah bint Abdulrahman University, Riyadh, Saudi Arabia.

Author contributions: H.O.T. – conceptualization, writing – original draft, supervision, writing – review and editing; G.A. – visualization, software, writing – original draft; H.M.H.Z. – formal analysis, data curation; G.K. – data curation, formal analysis, writing – original draft; E.I. – data curation, formal analysis, writing – original draft; D.S.B. – visualization, software; E.R. – visualization, software, A.E. – methodology, funding acquisition. (Author A.E. would like to thank "Dunarea de Jos" University of Galati, Romania, for the material and technical support).

Conflict of interest: None.

Ethical approval: The conducted research is not related to either human or animals use.

Data availability statement: The datasets generated during and/or analyzed during the current study are available from the corresponding author on reasonable request.

References

[1] Abdel Rahman RO, Hung YT. Application of ionizing radiation in wastewater treatment: an overview. Water. 2019;12(1):19. doi: 10.3390/w12010019.

[2] Vrijheid M, Cardis E, Ashmore P, Auvinen A, Bae JM, Engels H, et al. Mortality from diseases other than cancer following low doses of ionizing radiation: results from the 15-Country Study of nuclear industry workers. Int J Epidemiol. 2007;36(5):1126–35. doi: 10.1093/ije/dym138.

[3] Madureira J, Barros L, Cabo Verde S, Margaça FM, Santos-Buelga C, Ferreira IC. Ionizing radiation technologies to increase the extraction of bioactive compounds from agro-industrial residues: a review. J Agric Food Chem. 2020;68(40):11054–67. doi: 10.1021/acs.jafc.0c04984.
[4] Howe GR, Zablotska LB, Fix JJ, Egel J, Buchanan J. Analysis of the mortality experience amongst US nuclear power industry workers after chronic low-dose exposure to ionizing radiation. Radiat Res. 2004;162(5):517–26. http://www.jstor.org/stable/3581146.
[5] Karbownik M, Reiter RJ. Antioxidative effects of melatonin in protection against cellular damage caused by ionizing radiation. Proc Soc Exp Biol Med Minireviews. 2000;225(1):9–22. doi: 10.1177/153537020022500102.
[6] Rouif S. Radiation cross-linked polymers: recent developments and new applications. Nucl Instrum Methods Phys Res Sect B Beam Interact Mater At. 2005;236(1–4):68–72. doi: 10.1016/j.nimb.2005.03.252.
[7] Kerkmeijer LG, Fuller CD, Verkooijen HM, Verheij M, Choudhury A, MR-Linac Consortium Clinical Steering Committee, et al. The MRI-linear accelerator consortium: evidence-based clinical introduction of an innovation in radiation oncology connecting researchers, methodology, data collection, quality assurance, and technical development. Front Oncol. 2016;6:215. doi: 10.3389/fonc.2016.00215.
[8] Fenig E, Mishaeli M, Kalish Y, Lishner M. Pregnancy and radiation. Cancer Treat Rev. 2001;27(1):1–7. doi: 10.1053/ctrv.2000.0193.
[9] Little JB. Radiation carcinogenesis. Carcinogenesis. 2000;21(3):397–404. doi: 10.1093/carcin/21.3.397.
[10] Smith LE, Nagar S, Kim GJ, Morgan WF. Radiation-induced genomic instability: radiation quality and dose response. Health Phys. 2003;85(1):23–9. https://journals.lww.com/health-physics/Fulltext/2003/07000/Radiation_Induced_Genomic_Instability__Radiation.6.aspx.
[11] AbuAlRoos NJ, Amin NAB, Zainon R. Conventional and new lead-free radiation shielding materials for radiation protection in nuclear medicine: a review. Radiat Phys Chem. 2019;165:108439. doi: 10.1016/j.radphyschem.2019.108439.
[12] Crane GD, Abbott PV. Radiation shielding in dentistry: an update. Aust Dent J. 2016;61(3):277–81. doi: 10.1111/adj.12389.
[13] Ilik E. Effect of heavy rare-earth element oxides on physical, optical and gamma-ray protection abilities of zinc-borate glasses. Appl Phys A. 2022;128(6):1–10. doi: 10.1007/s00339-022-05642-6.
[14] Mattos GRS, Bordon CDS, Kassab LRP, Issa SA, ALMisned G, Tekin HO. Towards obtaining the optimum physical, optical and nuclear radiation attenuation behaviours of tellurite–-germanate glasses through Eu_2O_3 reinforcement: glass synthesis, experimental and theoretical characterisation study. Ceram Int. 2023;49(1):986–94. doi: 10.1016/j.ceramint.2022.09.072.
[15] ALMisned G, Zakaly HM, Ali FT, Issa SA, Ene A, Kilic G, et al. A closer look at the efficiency calibration of LaBr3 (Ce) and NaI (Tl) scintillation detectors using MCNPX for various types of nuclear investigations. Heliyon. 2022;8(10):e10839. doi: 10.1016/j.heliyon.2022.e10839.
[16] Kavaz E, Tekin HO, Zakaly HMH, Issa SAM, Kara U, Al-Buriahi MS, et al. Structural and gamma-ray attenuation properties of different resin composites for radiation shielding applications. Braz J Phys. 2022;52(5):1–9. doi: 10.1007/s13538-022-01157-w.
[17] Basgoz O, Guler O, Evin E, Yavuz C, ALMisned G, Issa SA, et al. Synthesis and structural, electrical, optical, and gamma-ray attenuation properties of ZnO-multi-walled carbon nanotubes (MWCNT) composite separately incorporated with CdO, TiO_2, and Fe_2O_3. Ceram Int. 2022;48(11):16251–62. doi: 10.1016/j.ceramint.2022.02.174.
[18] Sheyn DD, Racadio JM, Ying J, Patel MN, Racadio JM, Johnson ND. Efficacy of a radiation safety education initiative in reducing radiation exposure in the pediatric IR suite. Pediatric Radiol. 2008;38(6):669–74. doi: 10.1007/s00247-008-0826-9.
[19] Kim TH, Hong SW, Woo NS, Kim HK, Kim JH. The radiation safety education and the pain physicians' efforts to reduce radiation exposure. Korean J Pain. 2017;30(2):104–15. doi: 10.3344/kjp.2017.30.2.104.
[20] Wittkampf FH, Wever EF, Vos K, Geleijns J, Schalij MJ, Van der tol JAN, et al. Reduction of radiation exposure in the cardiac electrophysiology laboratory. Pacing Clin Electrophysiol. 2000;23(11):1638–44. https://onlinelibrary.wiley.com/doi/pdf/10.1046/j.1460-9592.2000.01638.x.
[21] Chang L, Zhang Y, Liu Y, Fang J, Luan W, Yang X, et al. Preparation and characterization of tungsten/epoxy composites for γ-rays radiation shielding. Nucl Instrum Methods Phys Res Sect B Beam Interact Mater At. 2015;356:88–93. doi: 10.1016/j.nimb.2015.04.062.
[22] Sayyed MI, Tekin HO, Altunsoy EE, Obaid SS, Almatari M. Radiation shielding study of tellurite tungsten glasses with different antimony oxide as transparent shielding materials using MCNPX code. J Non-Cryst Solids. 2018;498:167–72. doi: 10.1016/j.jnoncrysol.2018.06.022.
[23] Naseer KA, Marimuthu K, Al-Buriahi MS, Alalawi A, Tekin HO. Influence of Bi_2O_3 concentration on barium-telluro-borate glasses: physical, structural and radiation-shielding properties. Ceram Int. 2021;47(1):329–40. doi: 10.1016/j.ceramint.2020.08.138.
[24] Ruengsri S, Insiripong S, Sangwaranatee N, Kaewkhao J. Development of barium borosilicate glasses for radiation shielding materials using rice husk ash as a silica source. Prog Nucl Energy. 2015;83:99–104. doi: 10.1016/j.pnucene.2015.03.006.
[25] Ilik BO, Kilic G, Ilik E, Kavaz E, ALMisned G, Tekin HO. Elucidating the influences of Tantalum (V) oxide in Bi_2O_3–TeO_2–ZnO ternary glasses: an experimental characterization study on optical and nuclear radiation transmission properties of high-density glasses. Ceram Int. 2023;49(7):10906–13. doi: 10.1016/j.ceramint.2022.11.284.
[26] Chanthima N, Kaewkhao J. Investigation on radiation shielding parameters of bismuth borosilicate glass from 1 keV to 100 GeV. Ann Nucl energy. 2013;55:23–8. doi: 10.1016/j.anucene.2012.12.011.
[27] Tekin HO, ALMisned G, Rammah YS, Susoy G, Ali FT, Baykal DS, et al. The significant role of WO_3 on high-dense BaO–P_2O_3 glasses: transmission factors and a comparative investigation using commercial and other types of shields. Appl Phys A. 2022;128(6):1–11. doi: 10.1007/s00339-022-05620-y.
[28] Tashlykov OL, Vlasova SG, Kovyazina IS, Mahmoud KA. Repercussions of yttrium oxides on radiation shielding

capacity of sodium-silicate glass system: experimental and Monte Carlo simulation study. Eur Phys J Plus. 2021;136(4):1–17. doi: 10.1140/epjp/s13360-021-01420-0.
[29] Alalawi A. Experimental and Monte Carlo investigations on the optical properties and nuclear shielding capability of $Bi_2O_3Na_2O–B_2O_3Cu_2O$ glasses. J Non-Cryst Solids. 2020;548:120321. doi: 10.1016/j.jnoncrysol.2020.120321.
[30] Tuscharoen S, Kaewkhao J, Limsuwan P, Chewpraditkul W. Structural, optical and radiation shielding properties of $BaO–B_2O_3$–rice husk ash glasses. Procedia Eng. 2012;32:734–9. doi: 10.1016/j.proeng.2012.02.005.
[31] ALMisned G, Baykal DS, Kilic G, Susoy G, Zakaly HM, Ene A, et al. Assessment of the usability conditions of $Sb_2O_3–PbO–B_2O_3$ glasses for shielding purposes in some medical radioisotope and a wide gamma-ray energy spectrum. Appl Rheol. 2022;32(1):178–89. doi: 10.1515/arh-2022-0133.
[32] Tekin HO, Singh VP, Manici T. Effects of micro-sized and nano-sized WO_3 on mass attenauation coefficients of concrete by using MCNPX code. Appl Radiat Isotopes. 2017;121:122–5. doi: 10.1016/j.apradiso.2016.12.040.
[33] Elmahroug Y, Almatari M, Sayyed MI, Dong MG, Tekin HO. Investigation of radiation shielding properties for $Bi_2O_3–V_2O_5–TeO_2$ glass system using MCNP5 code. J Non-Cryst Solids. 2018;499:32–40. doi: 10.1016/j.jnoncrysol.2018.07.008.
[34] Kilic G, Ilik E, Issa SA, ALMisned G, Tekin HO. ZnO/CdO translocation in $P_2O_5–TeO_2–ZnO$ ternary glass systems: a reformative enhancement tool for physical, optical, and heavy-charged particles attenuation properties. Optik. 2022;268:169807. doi: 10.1016/j.ijleo.2022.169807.
[35] Li C, Zhang X, Onah VC, Yang W, Leng Z, Han K, et al. Physical and optical properties of $TeO_2–WO_3–GdF_3$ tellurite glass system. Ceram Int. 2022;48(9):12497–505. doi: 10.1016/j.ceramint.2022.01.116.
[36] Kılıç G, İşsever UG, İlik E. The synthesis and characterization of zinc-tellurite semiconducting oxide glasses containing Ta_2O_5. Mater Res Express. 2019;6(6):065907. doi: 10.1088/2053-1591/ab0b1e.
[37] Zhang X, Xu W, Zhang J, Huang P, Qi X. High-entropy oxide glasses $TiO_2–Ta_2O_2Nb_2O_5—WO_3–MO_x$ (M = La/Sm/Eu/Tb/Dy) with high refractive index. J Non-Cryst Solids. 2022;597:121862. doi: 10.1016/j.jnoncrysol.2022.121862.
[38] Ansari AA, Muthumareeswaran MR, Lv R. Coordination chemistry of the host matrices with dopant luminescent Ln^{3+} ion and their impact on luminescent properties. Coord Chem Rev. 2022;466:214584. doi: 10.1016/j.ccr.2022.214584.
[39] Maffei N, Prasad SE, Wheat TA. Electrical properties of $ZrF_4–BaF_2–GdF_3$-AlF_3-glass. J Mater Sci. 1991;26(12):3159–64, https://link.springer.com/content/pdf/10.1007/BF01124657.pdf.
[40] Mann KS, Mann SS. Py-MLBUF: development of an online-platform for gamma-ray shielding calculations and investigations. Ann Nucl Energy. 2021;150:107845. doi: 10.1016/j.anucene.2020.107845.
[41] Kilic G, Kavaz E, Ilik E, ALMisned G, Tekin HO. CdO-rich quaternary tellurite glasses for nuclear safety purposes: synthesis and experimental gamma-ray and neutron radiation assessment of high-density and transparent samples. Optical Mater. 2022;129:112512. doi: 10.1016/j.optmat.2022.112512.
[42] Issa SA, Tekin HO, Saudi HA, Koubisy MSI, Zhukovsky M, Ali AS, et al. Fabrication of newly developed tungsten III-oxide glass family: physical, structural, mechanical, radiation shielding effectiveness. Optik. 2022;259:169025. doi: 10.1016/j.ijleo.2022.169025.
[43] Sallam OI, Issa SAM, Rashad M, Madbouly AM, Tekin HO, Badawi A, et al. Impact of molybdenum on optical, structure properties and gamma radiation shielding parameters of borophosphate glass: intensive experiment investigations. Radiat Phys Chem. 2022;198:110140. doi: 10.1016/j.radphyschem.2022.110140.
[44] Issa SA, Rashad M, Hanafy TA, Saddeek YB. Experimental investigations on elastic and radiation shielding parameters of $WO_3–B_2O_3–TeO_2$ glasses. J Non-Cryst Solids. 2020;544:120207. doi: 10.1016/j.jnoncrysol.2020.120207.
[45] Baykal DŞ, Tekin HO, Mutlu RBÇ. An investigation on radiation shielding properties of borosilicate glass systems. Int J Comput Exp Sci Eng. 2021;7(2):99–108. doi: 10.22399/ijcesen.960151.
[46] Oruncak B. Gamma-ray shielding properties of Nd_2O_3 added iron–boron–phosphate based composites. Open Chem. 2022;20(1):237–43. doi: 10.1515/chem-2022-0143.
[47] Waheed F, İmamoğlu M, Karpuz N, Ovalıoğlu H. Simulation of neutrons shielding properties for some medical materials. Int J Comput Exp Sci Eng. 2022;8(1):5–8. doi: 10.22399/ijcesen.1032359.
[48] Boodaghi Malidarre R, Akkurt İ, Gunoglu K, Akyıldırım H. Fast neutrons shielding properties for HAP-Fe_2O_3 composite materials. Int J Comput Exp Sci Eng. 2021;7(3):143–5. doi: 10.22399/ijcesen.1012039.
[49] Akkurt I. Effective atomic numbers for Fe–Mn alloy using transmission experiment. Chin Phys Lett. 2007;24:2812. doi: 10.1088/0256-307X/24/10/027.
[50] Kurtulus R, Buriahi MS, Issa SAM, Tekin HO, Kavas T, Kavaz E. Physical, structural, mechanical and radiation shielding features of waste pharmaceutical glasses doped with Bi_2O_3. Optik. 2022;261:169108. doi: 10.1016/j.ijleo.2022.169108.
[51] Kurtuluş R, Kavas T, Kavaz E, Tekin HO, Kurucu Y. Synthesis and characterization of waste CRT glasses through physical, optical and structural properties: a comprehensive study on recycling. Optik. 2021;248:168167. doi: 10.1016/j.ijleo.2021.168167.
[52] Kurtulus R, Kavas T, Akkurt I, Gunoglu K, Tekin HO, Kurtulus C. A comprehensive study on novel alumino-borosilicate glass reinforced with Bi_2O_3 for radiation shielding applications: synthesis, spectrometer, XCOM, and MCNP-X works. J Mater Sci Mater Electron. 2021;32:13882–96. doi: 10.1007/s10854-021-05964-w.